ANTIMICROBIAL AGENTS AND CHEMOTHERAPY, Sept. 2008, p. 3385–3393 Vol. 52, No. 9
0066-4804/08/$08.00+0 doi:10.1128/AAC.01508-07

Identification and Biochemical Characterization of Small-Molecule Inhibitors of West Nile Virus Serine Protease by a High-Throughput Screen▽

Niklaus H. Mueller,[1] Nagarajan Pattabiraman,[2] Camilo Ansarah-Sobrinho,[3] Prasanth Viswanathan,[1] Theodore C. Pierson,[3] and R. Padmanabhan[1]*

Department of Microbiology and Immunology[1] and Department of Oncology,[2] Georgetown University Medical Center, Washington, DC 20057, and Viral Pathogenesis Section, Laboratory of Viral Diseases, NIAID, NIH, Bethesda, Maryland 20892[3]

Received 21 November 2007/Returned for modification 9 January 2008/Accepted 30 May 2008

West Nile virus and dengue virus are mosquito-borne flaviviruses that cause a large number of human infections each year. No vaccines or chemotherapeutics are currently available. These viruses encode a serine protease that is essential for polyprotein processing, a required step in the viral replication cycle. In this study, a high-throughput screening assay for the West Nile virus protease was employed to screen ~32,000 small-molecule compounds for identification of inhibitors. Lead inhibitor compounds with three distinct core chemical structures (1 to 3) were identified. In a secondary screening of selected compounds, two compounds, belonging to the 8-hydroxyquinoline family (compounds A and B) and containing core structure 1, were identified as potent inhibitors of the West Nile virus protease, with K_i values of 3.2 ± 0.3 μM and 3.4 ± 0.6 μM, respectively. These compounds inhibited the dengue virus type 2 protease with K_i values of 28.6 ± 5.1 μM and 30.2 ± 8.6 μM, respectively, showing some selectivity in the inhibition of these viral proteases. However, the compounds show no inhibition of cellular serine proteases, trypsin, or factor Xa. Kinetic analysis and molecular docking of compound B onto the known crystal structure of the West Nile virus protease indicate that the inhibitor binds in the substrate-binding cleft. Furthermore, compound B was capable of inhibiting West Nile virus RNA replication in cultured Vero cells (50% effective concentration, 1.4 ± 0.4 μM; selectivity index, 100), presumably by inhibition of polyprotein processing.

West Nile virus (WNV) and the four serotypes of dengue virus (DENV1 to DENV4) have recently emerged as significant human pathogens that cause millions of infections each year and result in considerable morbidity and mortality (16, 26). WNV was introduced into the Western Hemisphere during an outbreak in the United States in 1999. In the following years, WNV has spread throughout much of North America and has become a major public health concern (reviewed in reference 7). Most WNV infections are asymptomatic; however, about 20% of cases are associated with mild flu-like symptoms. A small fraction of these cases progresses to more-severe clinical manifestations, including encephalitis and/or flaccid paralysis. Currently, there are no approved vaccines or antiviral therapeutics available for WNV-infected humans.

The WNV genome consists of approximately 11 kb of RNA of positive polarity, which encodes a single polyprotein that is processed co- and posttranslationally by the host signal peptidase and the viral serine protease into at least 10 proteins. The three structural proteins, capsid (C), prM, and envelope (E), arise from the N terminus of the polyprotein, and the seven nonstructural (NS) proteins (NS1, NS2A, NS2B, NS3, NS4A, NS4B, and NS5) arise from the C-terminal portion during processing at the endoplasmic reticulum of the host cell (7, 23). The active form of the viral serine protease consists of a complex of two proteins, NS2B and NS3. NS3 is a multifunctional protein. The amino-terminal domain contains the serine protease catalytic triad, consisting of amino acid residues H51, D75, and S135 (5). This domain interacts with NS2B, a required cofactor, to form the active serine protease (3, 8, 9, 14, 15, 33, 35). Fine mapping of the minimal domain of NS3 has revealed that the amino-terminal 167 residues are sufficient for *cis*-cleavage at the NS2B-NS3 junction (22).

The two-component NS2B/NS3 viral serine protease activity plays a key role in flaviviral polyprotein processing. This is an obligatory step prior to viral RNA replication, thus identifying the viral serine protease as an excellent therapeutic target. The protease cleavage sites in the polyprotein have a pair of basic amino acids (R and K) at the P2 and P1 (occasionally there is a Q at P2) positions, followed by a short-chain amino acid (G, S, or A) at the P1′ position (30). NS2B is an endoplasmic reticulum integral membrane protein (12). It consists of a conserved hydrophilic domain (NS2BH) and three hydrophobic domains; the former is essential both for interaction with the NS3 protease domain (NS3-pro) and for protease activity (9, 12, 14).

In a previous study using peptide substrates, we reported that the interaction of DENV2 NS2BH with NS3-pro increased the k_{cat}/K_m of NS3-pro from ~3.3 × 10^3-fold to 7.6 × 10^3-fold (34). The crystal structures of the NS2BH cofactor bound to NS3-pro of WNV and DENV2 were reported recently, the former in the presence of a substrate-based inhibitor peptide covalently linked to the active site (1, 13). These structures revealed the identities of the amino acid residues

* Corresponding author. Mailing address: Department of Microbiology and Immunology, Georgetown University School of Medicine, 3900 Reservoir Rd. NW, Med-Dent SW309, Washington, DC 20057. Phone: (202) 687-2092. Fax: (202) 687-1800. E-mail: rp55@georgetown.edu.

▽ Published ahead of print on 7 July 2008.

involved in substrate recognition and provided a structural basis for the activation of NS3-pro by NS2BH. They also provided a rational explanation for the mutational effects of the WNV NS2BH cofactor as well as for its role in the active protease (10).

The goal of this study was to identify small-molecule inhibitors of the WNV protease. We employed previously described in vitro protease assays (27, 34) adapted to a high-throughput format. Further detailed biochemical and kinetic analyses of representative compounds led to the identification of two lead compounds (compounds A and B) that inhibited the WNV NS2BH/NS3-pro in vitro. Compound B was also found to inhibit WNV RNA replication in cultured cells when the replicon RNA was delivered by infection with WNV particles bearing replicon RNA (28). The kinetic data revealed that compound B functioned as a competitive inhibitor. This conclusion is supported by molecular modeling, which shows that there is only one plausible binding site for the compound within the NS3-pro domain in the vicinity of the substrate binding pockets.

MATERIALS AND METHODS

Materials. The high-throughput screening was done at Harvard Medical School National Screening Facility—ICCB, Longwood (Boston, MA). The compound libraries used in this study are NINDS Bioactives, Chemdiv 2, Maybridge 3, ICBG fungal extracts, Enamine 1, I.F. Lab 1, and Bionet 2. The seven compounds were purchased from the following sources. compound A from ChemDiv (vendor ID, 3460-0035), compound B from I.F. Lab (vendor ID, F0842-0004), compound C from ChemDiv (vendor ID, C145-0031), compound D from I.F. Lab (vendor ID, F0318-0154), compound E from ChemDiv (vendor ID, 3455-0283), compound F from Maybridge (vendor ID, SP 01197), and compound G from ChemDiv (vendor ID, C651-0606).

Expression of WNV and DENV2 NS2BH/NS3-pro in *Escherichia coli* and purification. Procedures for the expression and purification of WNV (strain EG101) and DENV2 (strain New Guinea C) cofactor NS2BH/NS3 protease complexes were similar to those described elsewhere (27, 34). Briefly, *E. coli* Top10 F′ cells (Invitrogen, Carlsbad, CA) were transformed with the protease expression plasmid. Cells were grown at 37°C until the optical density at 600 nm was ~0.5. Cells were then induced with 0.5 mM isopropyl-1-thio-β-D-galactopyranoside (American Bioanalytical, Natick, MA) and incubated for 4 h at 37°C. Cells were harvested by centrifugation (5,000 × *g*) for 15 min at 4°C, washed once with a buffer containing 50 mM Tris-HCl (pH 7.5) and 200 mM NaCl, centrifuged at 5,000 × *g* for 15 min at 4°C, and stored at −80°C until use.

Proteases were purified by suspending bacterial pellets in 50 mM HEPES (pH 7.0)–500 mM NaCl (buffer A) with 0.05 mg/ml lysozyme. Cells were incubated for 30 min on ice after addition of a 10% stock solution of Triton X-100 (final concentration, 0.5%). Cells were disrupted by sonication for 2 min, and the soluble fraction was collected after centrifugation (15,000 × *g*) for 30 min at 4°C. The soluble fraction was incubated for 1 h at 4°C with Talon resin (BD Bioscience, San Jose, CA), which was preequilibrated in buffer A. The affinity resin was centrifuged at 400 × *g* for 10 min at 4°C, washed three times with buffer A, and packed into a column. Washing of the column was continued with buffer A containing 10 mM imidazole, followed by elution of the protease with buffer A containing 150 mM imidazole. The protease was concentrated and further purified by Sephadex G-75 gel filtration chromatography. The purified protease fractions were pooled and dialyzed against 1 liter of a buffer containing 50 mM Tris-HCl (pH 7.5) and 300 mM NaCl, with four changes of dialysis buffer. Aliquots (100 μl) were frozen at −80°C.

HTS protease assay. Our previously reported protease assays (100 μl) (27, 34) were adapted for a 384-well plate format (30.1 μl). High-throughput screening (HTS) assays were performed at the National Screening Laboratory for the Regional Centers of Excellence in Biodefense and Emerging Infectious Diseases (NSRB, Boston, MA). Microtiter plates were loaded sequentially with 14 μl of the reaction buffer containing 200 mM Tris-HCl (pH 9.5) and 30% glycerol (TG buffer) using the automated Wellmate (Matrix, Hudson, NH) and with 6 μl of WNV protease (0.05 μM) in TG buffer containing 15 mM NaCl (3 mM final concentration). Plates were then centrifuged at 1,000 × *g* for 3 min at room temperature to mix samples and pool liquids at the bottoms of the wells. Inhibitor compounds (100 nl [5 mg/ml] in dimethyl sulfoxide [DMSO]) were added to each well in duplicate by a pin transfer mechanism of a robotic delivery system. The final inhibitor concentrations in the assays varied due to different molecular weights of the compounds screened in the primary HTS. Plates were incubated at room temperature to allow for formation of protease-inhibitor complexes. The fluorogenic substrate *t*-butyl-oxycarbonyl (Boc)-Gly-Lys-Arg-7–amino-4-methyl coumarin (AMC) (10 μl in TG buffer; final concentration in the reaction mixture, 50 μM) was added using the Wellmate, and the plates were centrifuged for 3 min at 1,000 × *g* and incubated at room temperature for 15 min. Fluorescence was measured at excitation and emission wavelengths of 385 nm and 465 nm, respectively, on a Perkin-Elmer (Waltham, MA) spectrofluorometer. To validate the assay conditions, aprotinin (bovine pancreatic trypsin inhibitor [BPTI]) was used as a positive control. Assay mixtures containing DMSO were used as negative controls. The average of fluorescence values in duplicate wells for a given compound was used to determine the percentage of activity by taking the values obtained with DMSO controls as 100%. Compounds that reduced the protease activity by ≥50% were selected for further analysis.

Further analyses of protease inhibitor compounds. Compounds selected from the HTS were further analyzed by in vitro protease assays performed in opaque 96-well plates. The enzyme kinetics was done under steady-state conditions. Standard reaction mixtures (50 μl) containing 200 mM Tris-HCl (pH 9.5), 6 mM NaCl, 30% glycerol, 67 nM either DENV2, WNV protease, or trypsin or 25 nM factor Xa (New England Biolabs, Ipswich, MA), and 50 μM inhibitor in each assay were incubated for 15 min at room temperature. Reactions were started by the addition of the substrate Boc-Gly-Lys-Arg-AMC for the WNV protease, Boc-Gly-Arg-Arg-AMC for the DENV2 protease, benzyloxycarbonyl (Z)-Gly-Pro-Arg-*para*-nitroanilide for trypsin, or Boc-Ile-Glu-Gly-Arg-AMC for factor Xa (Bachem, Torrance, CA), each at a final concentration of 100 μM, and incubation was carried out at room temperature for 15 min. The absorbance of each well containing *para*-nitroaniline was measured at 405 nm using a spectrophotometer (Molecular Devices, Sunnyvale, CA). The fluorescence of AMC released from the WNV or DENV2 substrate was measured using a Tecan Geneios (Durham, NC) spectrofluorometer at excitation and emission wavelengths of 390 nm and 465 nm, respectively. Similarly, the WNV protease activity was determined using the fluorogenic tetrapeptide substrate containing the P4-to-P1 residues and the fluorogenic group 4-methoxy-β-naphthylamide (MNA) at the P1′ position (Z-Val-Lys-Lys-Arg-MNA). Fluorescence was measured using a spectrofluorometer (Molecular Devices) at excitation and emission wavelengths of 290 and 420 nm, respectively. Fluorescence values obtained with the no-inhibitor control were taken as 100%, and those in the presence of inhibitors were plotted as the percentage of inhibition of the control using Microsoft Excel.

To determine the K_i of an inhibitor, assays were performed using standard conditions as follows. Four different inhibitor concentrations and a no-inhibitor control (0 to 5 μM) were each assayed at eight or more substrate concentrations ranging from 50 to 1,000 μM. In each assay, the enzyme and inhibitor were incubated at room temperature for 15 min, followed by the addition of the substrate. The reactions were allowed to continue for an additional 15 min before measurement of fluorescence. The fluorescence values were converted to micromoles per minute of AMC (or MNA) using a standard curve, and the K_i values were determined using SigmaPlot (version 8.0) with a kinetics module (version 1.1). All assays were done in triplicate.

Inhibition of WNV RNA replication in Vero cells. Inhibition of WNV RNA replication was measured following infection of Vero cells with WNV reporter virus particles (RVPs), which encapsidate the WNV subgenomic replicon encoding the *Renilla* luciferase reporter. The construction of the replicon and methods for RVP production are described elsewhere (28). Briefly, WNV-RVPs were produced by transfecting DNA expression plasmids that encoded virus structural proteins (C, prM, and E) into a baby hamster kidney (BHK-21) cell line that stably expressed the WNV subgenomic replicon. RVPs were harvested at 48 h and frozen at −80°C. The titer of the RVP stock was determined on Vero cells (28). The titers of WNV RVPs are typically 0.5×10^6 to 1.0×10^6 per ml. The appropriate amount of RVPs to be added to Vero cells was determined from the linear plot of RVP input versus luciferase signal. Infections were performed with 200 μl of a 1-to-5 dilution of these stocks (approximately 1×10^4 RVPs at a multiplicity of infection of 0.5 to 1.0). To measure the inhibition of replication, Vero cells were pretreated with twofold serial dilutions of compound B in minimal essential medium–10% fetal bovine serum–1% penicillin-streptomycin (complete minimal essential medium). Thirty minutes after the addition of the drug, 200 μl of WNV-RVPs was added to the cells. RVP-infected cells were harvested at 48 h postinfection, lysed, and assayed for the luciferase signal according to the manufacturer's instructions (Promega, Madison, WI). The resulting data were analyzed using a least-squares minimization nonlinear regression approach to derive a sigmoidal dose-response curve with a variable slope

(GraphPad Prism, San Diego, CA). The 50% effective concentration (EC_{50}) corresponds to the concentration of drug required to inhibit infection by 50%.

To determine the toxicity of compounds for mammalian cells, Vero cells were plated in 96-well black-walled microtiter plates with flat, clear bottoms at a density of 5,000 cells/well. Cells were incubated for 24 h at 37°C in a 5% CO_2 incubator. The indicated concentrations of compound B were prepared in Dulbecco's modified Eagle's medium in 10% fetal bovine serum, added to the wells in triplicate, and incubated further for 24 h. The viable cells were detected by a CellTiter-Glo assay kit (Promega) according to the manufacturer's instructions, and the percentage of cytotoxicity was calculated in comparison to the values obtained from 100% viable cells in no-compound control wells.

Molecular docking. The coordinates for the crystal structure of WNV (PDB ID 2FP7) protease with the activating peptide (NS2BH) (13) were used for molecular docking of the inhibitor compound B. The kinetic data revealed a competitive mode of inhibition of the WNV protease by compound B. Therefore, for molecular docking of the inhibitor compound, the substrate-based inhibitor peptide was removed from the crystal structure of WNV protease, since the substrate and inhibitor binding sites presumably would overlap. The FlexX module of Sybyl 7.0 (Tripos, St. Louis, MO) was used to dock compound B into the substrate-binding pocket. Since compound B has a chiral carbon, we docked both enantiomers. For each enantiomer, a total of 50 energetically favorable conformations of compound B were generated for molecular docking. We rank-ordered these complexes based on the FlexX scoring functions. The top 10 favorable complexes were then subjected to full energy minimization using the DISCOVER forcefield (Accelrys Inc., San Diego, CA). The complex with the lowest binding energy was selected for further analysis.

RESULTS AND DISCUSSION

Identification of inhibitors of the WNV protease by HTS. The flavivirus protease is required for processing of the polyprotein precursor prior to viral RNA replication and therefore is an excellent target for the development of antiviral therapeutics. In this study, we sought to identify small-molecule inhibitors of the WNV protease. We screened 32,337 compounds from seven different libraries as described in Materials and Methods. This primary HTS gave rise to 212 compounds that inhibited WNV protease activity by ≥50% (Fig. 1A).

To select for compounds with drug-like physicochemical and pharmacological properties, defined as "Lipinski's rule of five" (24), compounds identified in the HTS assay were next sorted in silico using several different filters. The compounds were selected based on potency (being active at ≤50 μM) and mass (molecular size, <500 Da). To this list of compounds, additional filters were applied for selection (24) (Fig. 1A). Compounds that met the following criteria were selected: (i) the calculated value of the logarithm of the octanol-water partition coefficient was lower than 5 (this C log P value is a determinant of the solubility of the compound in aqueous media); (ii) the sum of the numbers of nitrogen and oxygen atoms (H-bond acceptors) was less than 10; (iii) there were fewer than five H-bond donor atoms and fewer than 10 rotatable bonds (to eliminate compounds that were too flexible); and (iv) the compounds contained peptide-like (NH—C═O) bonds, which would mimic protease substrates and likely bind to or near the active site of the protease. Finally, compounds containing reactive groups (such as C≡N, S—H) that could covalently modify the amino acid side chains of protease were eliminated.

Based on these criteria, we obtained 98 compounds (0.003% of the total number screened) that were divided into five groups based on structural similarity. For example, two groups of compounds have substituted quinoline rings (R1) that are linked to either an —NH—C═O or an —NH— group (core 1 [Fig. 1B]). The compounds with core 2 are also assigned to two groups depending on whether —NH—C═O is part of a five-member or a six-member ring. The core 3 compounds have the —NH—C═O moiety linked to a wide variety of R1 and R2 groups in chain-like structures. The range of the percentages of inhibition of these 98 compounds in five groups is shown in Table 1. Seven representative members of three core structures exhibiting high (78 to 86%), medium (66 to 72%), and low (52 to 63%) percentages of inhibition in the primary HTS were readily available from commercial sources (Fig. 2); of these seven compounds, three each had cores 1 (compounds A, B, and D) and 3 (compounds C, F, and G), and one compound had core 2 (E).

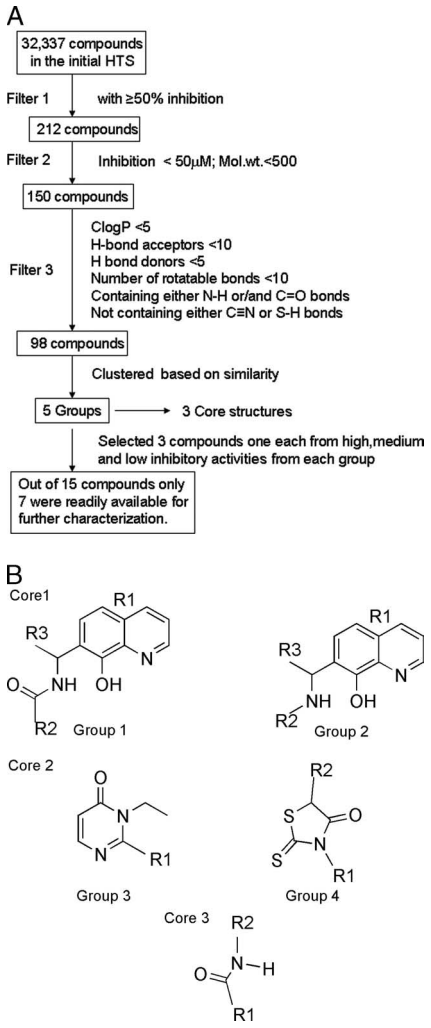

FIG. 1. (A) Flow chart for the primary HTS and secondary assays. The HTS identified 212 compounds, of which 150 compounds were selected after the indicated filters were applied. Additional criteria (filter 3) were applied for the selection of 98 compounds, which were clustered into five groups based on their chemical structures. Three compounds from each of the five groups with high, medium, and low inhibitory activities were selected, and seven commercially available compounds from this list were obtained for further analysis. (B) General structures of the three cores and five groups into which the 98 compounds were clustered. The ranges of inhibitory activities of these compounds are given in Table 1.

TABLE 1. Range of percentages of inhibition of 98 compounds identified by the HTS[a]

Compound core	Compound group	Range of inhibition (%)
1	1	86–75.0
1	2	86–52
2	3	83–51
2	4	83–50
3	5	72–50

[a] To determine the percentage of inhibition, HTS assays were performed in 384-well plates as described in Materials and Methods. The percentages of inhibition of 98 compounds are averages of duplicate readings. The general structures of the three cores and five groups are shown in Fig. 1B.

Dose-dependent inhibition of WNV protease by selected compounds. The seven compounds were analyzed for inhibition of the WNV and DENV2 proteases in vitro (Fig. 3A and B, respectively). Compounds with core 1, especially compounds A and B, exhibited the highest inhibition of the proteases. The K_i values of compounds A and B for the WNV protease were determined to be 3.2 ± 0.34 μM and 3.4 ± 0.59 μM, respectively (Table 2). Both compounds were approximately 10-fold less effective in the assay performed with the DENV2 protease and its preferred substrate, Boc-Gly-Arg-Arg-AMC (Table 2). These results suggest that since the original HTS was done using the WNV protease, the selected compounds show some selectivity toward WNV protease over DENV2 protease in the secondary screen. DENV2 and WNV belong to different serocomplex subgroups; the former is one of four dengue viruses, DENV1 to DENV4, in a distinct subgroup, and the latter belongs to the Japanese encephalitis virus serocomplex group, which includes Japanese encephalitis virus, St. Louis encephalitis virus, and Murray Valley encephalitis virus (23). The NS2B cofactor and the NS3-pro domains of these two subgroups of flaviviruses, in addition to having invariant amino acid residues, show greater sequence identity among members of the same subgroup than among members of different subgroups. In comparison to the potencies of compounds A and B, the single compound with core 2 (compound E) displayed only modest inhibition of either protease (Fig. 3), and therefore it was not pursued further. Compound C, with core 3 (Fig. 2), inhibited WNV protease by ~71% in the presence of its preferred substrate, Boc-Gly-Lys-Arg-AMC (Fig. 3A), with a K_i of 37.3 ± 6.4 μM (Table 2). However, it was twofold more effective against the DENV2 protease in the presence of its preferred substrate, Boc-Gly-Arg-Arg-AMC, with a K_i of 17.0 ± 4.3 μM. The amino acid sequences in the carboxy-terminal regions of the NS2BH cofactor domains of DENV2 and WNV proteases differ (an alignment is shown in Fig. 3C). Since this region plays a key role in the substrate specificities of the proteases (N. Mueller and R. Padmanabhan, unpublished data), it may explain the differences in the preference of amino acid residue at the P2 positions of the substrates and the inhibition profiles for these two proteases. Since the K_i values of compound C were in the range of 17 to 37 μM for both proteases, it was not analyzed further in the cell-based assay (see below).

Inhibition of WNV RNA replication by compound B. To extend our biochemical studies, we evaluated the abilities of the most potent inhibitors to block WNV RNA replication in cultured cells. First, compounds A and B were evaluated for their cytotoxicities on Vero cells using a luciferase-based assay that measures ATP in living cells. Compound B exhibited moderate cytotoxicity toward Vero cells in culture over the concentration range tested (cytotoxic concentration that reduced the viable cell count by 50% [CC_{50}], 140 ± 1.98 μM) (Fig. 4). On the other hand, compound A exhibited significantly higher cytotoxicity toward Vero cells over a wider range of drug concentrations tested (data not shown). To avoid the complications of the cytotoxicity of compound A for the interpretation of inhibition data, cell culture-based experiments were performed with compound B. *Renilla* luciferase-expressing WNV replicons packaged into RVPs were used for infection, followed by the measurement of the reporter activity to assess the efficacy of compound B.

Subgenomic flavivirus replicons that encode reporter genes have been developed and used in the identification of *cis*- and *trans*-acting factors (2, 19–21, 28, 32) and for characterization of antiviral compounds and neutralizing antibodies (17, 25, 28, 29). In this study, we used, for the first time, the WNV RVPs for evaluation of WNV protease inhibitor potency by infection of mammalian cells in the presence and absence of the inhibitor compound. The advantages of using this approach are that the RVPs are virus particles produced by complementation of a WNV replicon with the virus structural proteins in *trans*, and therefore, these experiments can be carried out under biosafety level-2 containment conditions. Moreover, the WNV replicon RNA, delivered into the cytoplasm by infection of cells with RVPs, initiates a cascade of events such as translation, polyprotein processing, assembly of the viral replicase complex, and viral RNA replication. Since an inhibitor of the viral protease is expected to interfere with polyprotein processing, affecting all subsequent steps, its potency could be assessed precisely by monitoring reporter gene expression as a function of inhibitor concentration. Vero cells were treated with serially diluted compound B and infected with RVPs. At 48 h postinfection, cells were harvested, and the luciferase activity was measured at each inhibitor concentration (Fig. 5A). From these analyses, the EC_{50} was determined to be 1.4 ± 0.3 μM,

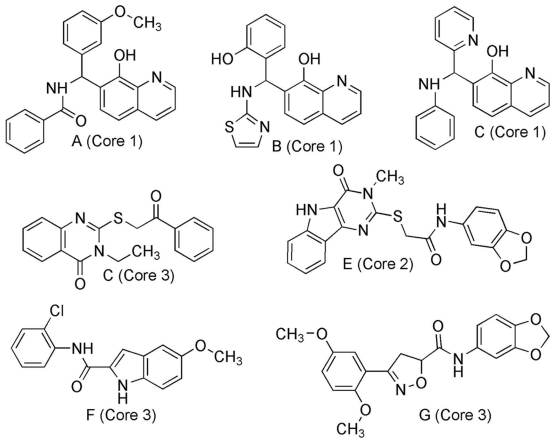

FIG. 2. Structures of the compounds selected for validation of the HTS. The structures of the seven compounds (compounds A to G) that were selected for further analysis are identified with their respective core structures.

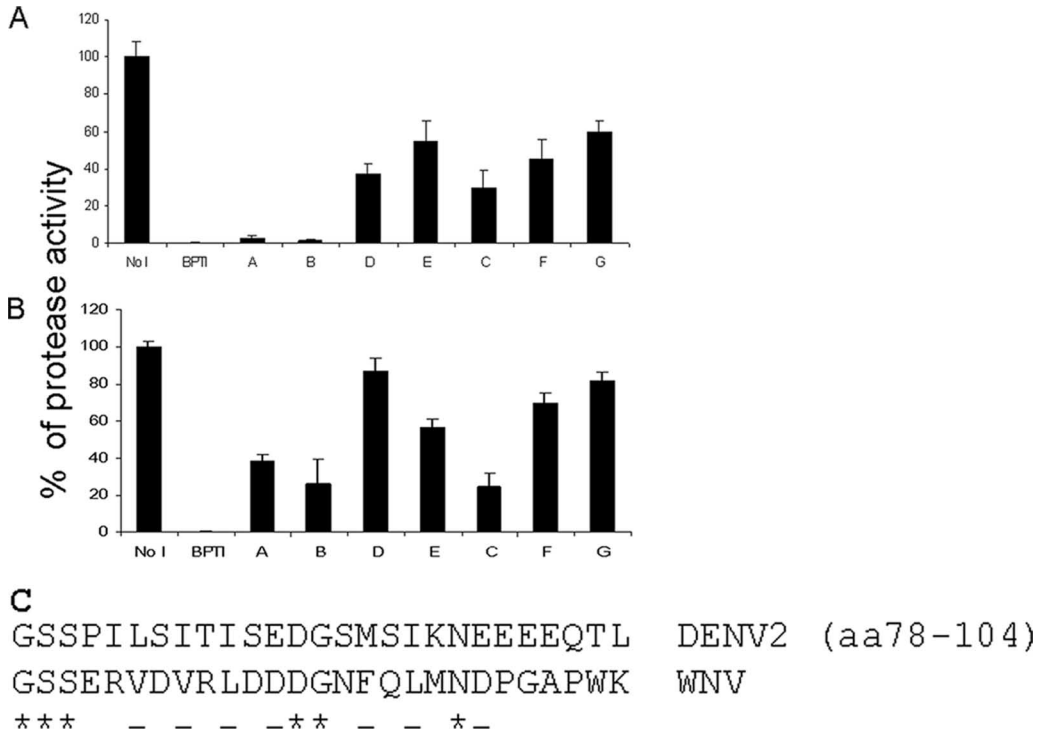

FIG. 3. (A and B) Inhibition of WNV and DENV2 proteases by selected compounds. The inhibitory potencies of seven selected compounds were determined using the WNV (A) and DENV2 (B) proteases. No I, no-inhibitor control (0.1% DMSO); BPTI, aprotinin (100 μM), used as a positive control. Letters below the third to seventh bars correspond to compounds A (core 1), B (core 1), D (core 1), E (core 2), C (core 3), F (core 3), and G (core 3). Compounds A to G were used at 50 μM in each assay. The error bars indicate standard deviations of the means from experiments performed in triplicate. (C) Differences between the amino acid sequences in the carboxy-terminal regions of the NS2BH cofactor domains of DENV2 and WNV proteases. This region is important for the formation of a substrate binding pocket on the NS3 protease domain (N. Mueller and R. Padmanabhan, unpublished data). Asterisks indicate identical amino acids; dashes indicate conservative amino acid substitutions.

and the selectivity index was 100. Similar results were obtained when cells were harvested at 24 or 72 h postinfection (Fig. 5B).

Kinetic analysis of inhibition by compound B. Next, we sought to determine the mode of inhibition of the WNV protease activity by compound B by following the kinetics of inhibition (Fig. 6). For these experiments, we used the fluorogenic tetrapeptide substrate Z-Val-Lys-Lys-Arg-MNA for the WNV protease assay. The WNV protease has a threefold-lower K_m for Z-Val-Lys-Lys-Arg-MNA than for the tripeptide substrate Boc-Gly-Lys-Arg-AMC (171.9 ± 6.2 μM versus 737 ± 150 μM, respectively [data not shown]). When the inhibitor concentrations were gradually increased, there was a

TABLE 2. K_i values of inhibitors

Compound	K_i (μM)[a]	
	DENV2-pro	WNV-pro
A (core 1)	28.6 ± 5.1	3.2 ± 0.3
B (core 1)	30.2 ± 8.6	3.4 ± 0.6
C (core 3)	17.0 ± 4.3	37.3 ± 6.4

[a] To determine the K_i of an inhibitor, assays were performed using standard conditions as described in Materials and Methods. For each compound, four different inhibitor concentrations and a no-inhibitor control (0 to 5 μM) were each assayed at eight or more substrate concentrations ranging from 50 to 1,000 μM. All assays were conducted in triplicate. Data are means ± standard deviations. DENV2-pro, DENV2 NS2BH/NS3-pro; WNV-pro, WNV NS2BH/NS3-pro.

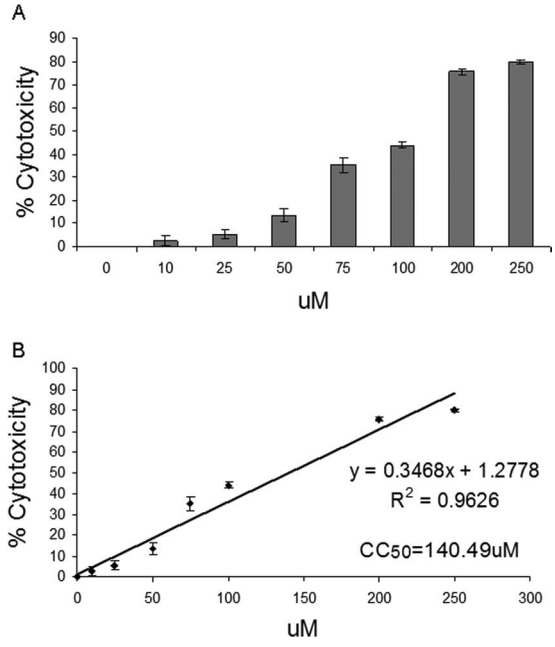

FIG. 4. The cytotoxicity of compound B for Vero cells was determined as described in Materials and Methods. (A) Percentages of cytotoxicity of compound B in Vero cells. The concentrations of compound B are shown along the *x* axis. Error bars represent standard deviations. Two independent experiments, each performed in triplicate, gave similar results. (B) CC_{50} derived from data in panel A.

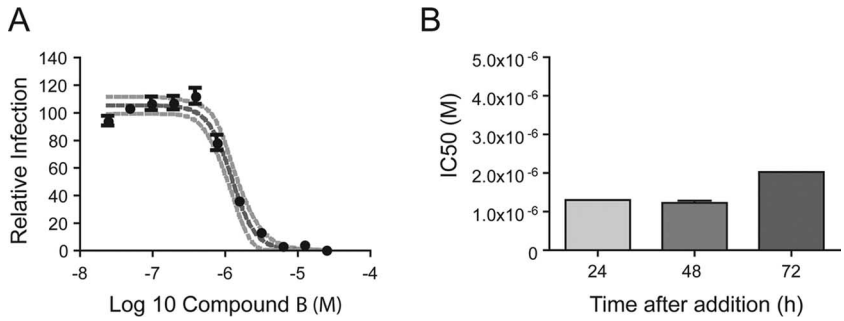

FIG. 5. (A) The inhibition of WNV RNA replication by compound B was measured by infection of Vero cells with RVPs as described in Materials and Methods. The *y* axis represents the *Renilla* luciferase activities of cell lysates as percent relative infection. The data were analyzed by nonlinear regression using GraphPad Prism (solid line). The dashed lines represent the 95% confidence interval of this analysis. Error bars indicate the standard errors of the means for experiments done in triplicate. Results are shown at 48 h after infection with RVPs. (B) Plot of EC_{50}s at 24, 48, and 72 h postinfection.

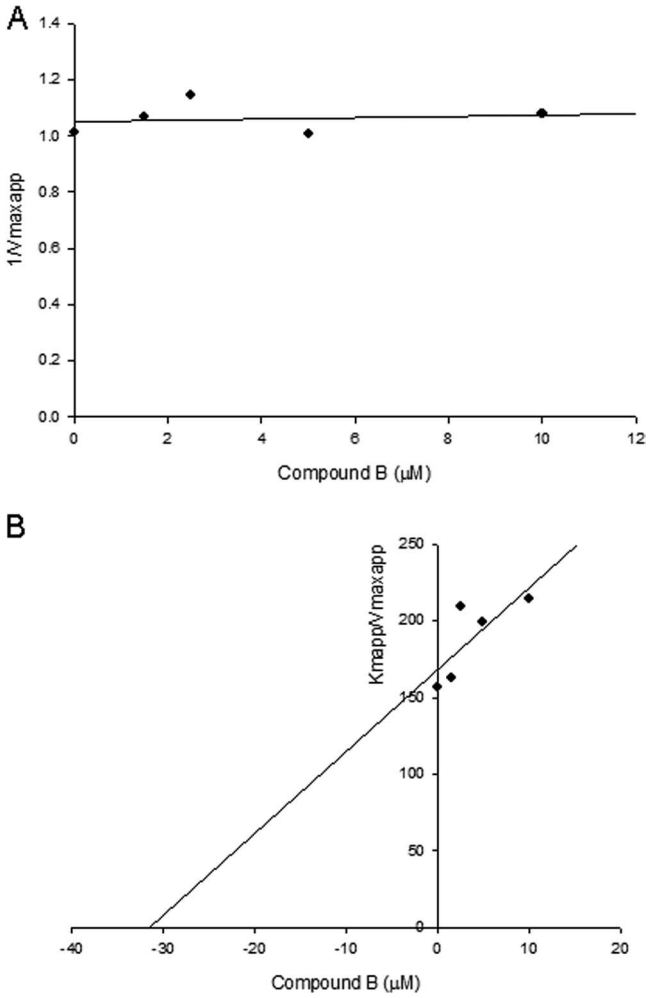

FIG. 6. Kinetics of inhibition of WNV protease by compound B. WNV protease assays were performed at various inhibitor concentrations (0, 1.5, 2.5, 5, and 10 μM) and substrate concentrations (10, 25, 50, 100, 150, 200, 300, and 400 μM) as described in Materials and Methods. The values were plotted using SigmaPlot, version 8.0, with a kinetic module (version 1.1). (A) Plot of the reciprocal values of apparent V_{max} ($1/V_{max}^{app}$) against the concentration of compound B. (B) Plot of K_m^{app}/V_{max}^{app} against the concentration of compound B. The units for V_{max}^{app} are μM/min; the K_m^{app} and inhibitor concentrations are micromolar concentrations. The experiments were repeated three times with similar results. Results of a representative experiment are shown.

concomitant increase in the apparent K_m/apparent V_{max} (K_m^{app}/V_{max}^{app}) ratios, while the values of V_{max}^{app} remained essentially constant (Fig. 6). The results in Fig. 6 also indicated a dose-dependent increase in the K_m^{app} values of the protease for the substrate with increasing concentrations of the inhibitor, signifying that the inhibitor interferes with the substrate affinity of the enzyme. These results are consistent with the conclusion that compound B inhibits the enzyme in a competitive manner. Similar results were obtained with the tripeptide substrate Boc-Gly-Lys-Arg-AMC (data not shown).

Next, we examined whether compounds A, B, and C (Fig. 2) could inhibit cellular serine proteases such as trypsin and factor Xa. We assayed trypsin using the chromogenic peptide substrate Z-Gly-Pro-Arg-pNA, the optimal P1 and P2 residues for trypsin (4), and we used the fluorogenic peptide substrate Boc-Ile-Glu-Gly-Arg-AMC for factor Xa under the conditions described under Materials and Methods. The compounds

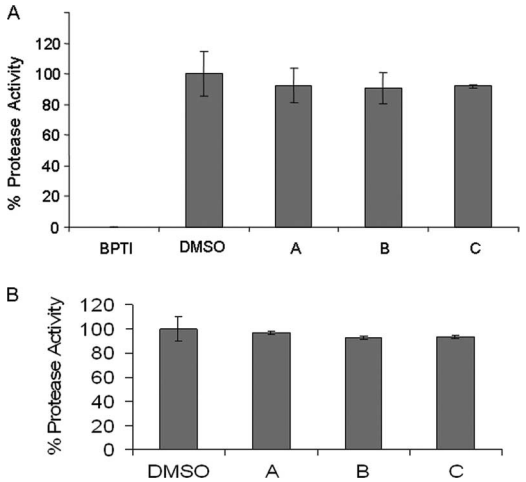

FIG. 7. Effects of compounds against trypsin and factor Xa. The effects of compounds A, B, and C (50 μM) on the protease activity of trypsin (A) or factor Xa (B) were determined using a chromogenic peptide substrate, Z-Gly-Pro-Arg-pNA (for trypsin), or a fluorogenic peptide substrate, Boc-Ile-Glu-Gly-Arg-AMC (for factor Xa), as described in Materials and Methods. Aprotinin was used as a positive control. Error bars indicate the standard deviations of the means for experiments done in triplicate.

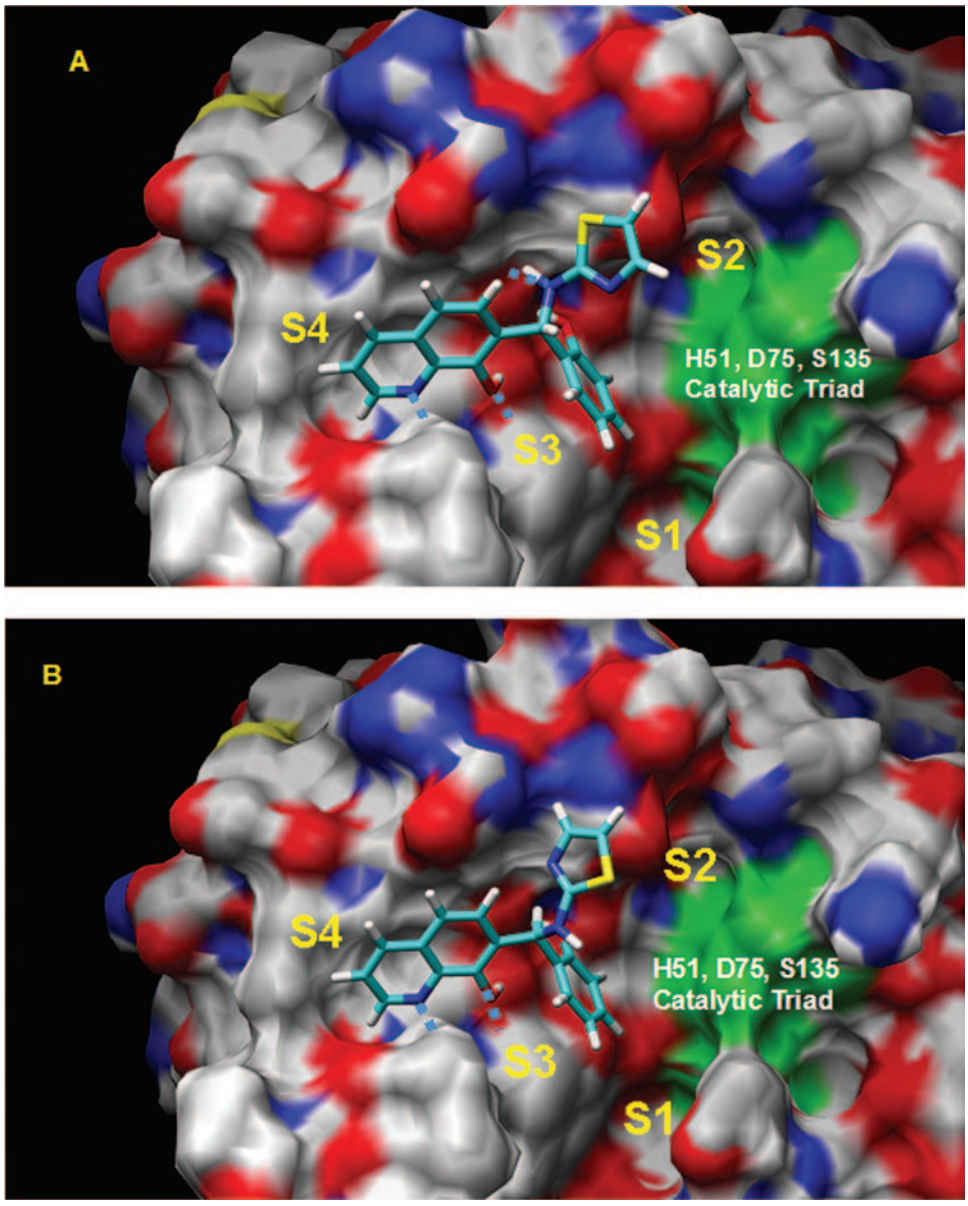

FIG. 8. Molecular docking of compound B onto WNV protease. The WNV protease crystal structure coordinates (PDB ID code 2FP7) were used for molecular docking. The solvent-accessible surface of the protein is shown in color-coded atoms (white, carbon; red, oxygen; blue, nitrogen). The catalytic triad (H51, D75, and S135) is shown as a green surface. Compound B is represented by a stick model. Cyan, C-C bond; red, yellow, and blue, C-O, C-S, and C-N bonds, respectively. (A) R enantiomer; (B) S enantiomer. The S1, S2, S3, and S4 pockets of the WNV protease are labeled. The H bonds are shown as dotted lines.

had essentially no inhibitory effect against trypsin or factor Xa (Fig. 7).

Molecular docking of lead compound B into the WNV protease. The crystal structures of the WNV protease with the NS2B cofactor peptide and substrate-based inhibitor peptide or the trypsin inhibitor aprotinin have been reported recently (1, 13). We used the crystal structure coordinates reported by Erbel et al. (13) for identifying the potential binding site of compound B in order to provide an explanation for its competitive mode of inhibition (Fig. 6). Compounds within the core structure 1 groups contain a hydroxyl moiety separated by four carbons covalently bonded to an —NH— group (Fig. 1B). These compounds could potentially form hydrogen bonds with residues of the S2-to-S4 pockets similarly to the substrate (Fig. 8). Compounds A and B, belonging to core structure 1 groups (Fig. 2), contain one chiral center with the potential to interact with the WNV protease, although the binding energy of the S enantiomer is less favorable (~6 kcal/mol) than that of the R form. The R enantiomer of compound B forms three hydrogen bonds with the protease (Fig. 8A). Two of these come from the nitrogen atom and the hydroxyl group in the 8-hydroxylquinoline moiety of compound B to form hydrogen bonds with the backbone nitrogen of I155 and with the backbone carbonyl oxygen of G153, respectively. The third hydrogen bond is

formed between the backbone carbonyl oxygen of F85 and the nitrogen atom that connects the five-member ring of compound B with other rings. These three hydrogen bonds stabilize the interaction of compound B with the substrate-binding pockets of the protease. In contrast to the R form, the S enantiomer of compound B forms only two hydrogen bonds (Fig. 8B). The two hydrogen bonds formed by the nitrogen atom and hydroxyl group in the 8-hydroxylquinoline moiety of compound B with I155 and G153 are similar to those of the R form of the compound. The third hydrogen bond present in the R enantiomer is not formed in the S form. Furthermore, differences in energy between the two enantiomers are due to the slightly unfavorable van der Waals interaction energy between the sulfur-containing five-member ring and the protease, as can be seen from the orientation of the ring. Amino acid residues that are in close proximity (less than 6 Å) to atoms of compound B include R78, D80, D82, N84, F85, Q86, and L87 of NS2BH and H51, T132, G151, N152, G153, V154, I155, M156, P157, and Y161 of NS3-pro. According to this docking model, both enantiomers interact with NS2BH as well as with NS3-pro, which could block substrate binding to the protease and thus inhibit the protease activity. Compound C, due to the presence of three fused rings, docks in a different orientation from those of compounds A and B, and its interaction energy with protease is less favorable than theirs. While docking studies indicate that compound B forms two or three hydrogen bonds with atoms in the backbone of amino acids G153, I155, and F85, structural studies are needed to confirm these data. The information gained from such structural studies is likely to shed light on whether there is any preference of one enantiomer over the other for inhibition of the enzyme.

HTS provides a powerful complement to structure-based rational design of small-molecule inhibitors of proteases, as is evident from the success of this approach in the identification of inhibitors of sudden acute respiratory syndrome coronavirus (6) and human immunodeficiency virus type 1 proteases (11, 31). This study reports an in vitro HTS assay for the WNV protease that led to the identification of inhibitors with a common core structure that inhibit the enzyme with K_i values in the low micromolar range and inhibit RNA replication in cultured cells with a low EC_{50}. Recently, in another study, HTS was employed to identify inhibitors of WNV protease activity. These compounds, in contrast to the results of our study, seemed to inhibit the interaction between the NS2B cofactor and the NS3-pro domain in an uncompetitive manner (18). Additional experiments on intracellular protein processing and resistance selection may be necessary to confirm the protease as the target of these compounds. Further work is necessary to optimize the lead compounds identified in this study by a structure-activity relationship approach, WNV infectivity assays, and viral protein expression. The HTS assay described in this study could be applied for identification of small-molecule inhibitors of other flaviviral proteases.

ACKNOWLEDGMENTS

The work was supported by grants AI57705 and AI070791 from NIH and by a Development grant from MARCE (AI-02-031) awarded to Myron Levine (U54 AI57168) and in part by the Intramural Research Program of the NIH, National Institute of Allergy and Infectious Diseases (NIAID).

We thank the faculty and staff of the New England Regional Center of Excellence (NSRB), including Su Chiang, Stewart Rudnicki, Dara Greenhouse, Sean Johnston, and Katrina Schulberg, for help in the use of the HTS facility.

REFERENCES

1. **Aleshin, A. E., S. A. Shiryaev, A. Y. Strongin, and R. C. Liddington.** 2007. Structural evidence for regulation and specificity of flaviviral proteases and evolution of the *Flaviviridae* fold. Protein Sci. **16:**795–806.
2. **Alvarez, D. E., A. L. De Lella Ezcurra, S. Fucito, and A. V. Gamarnik.** 2005. Role of RNA structures present at the 3′UTR of dengue virus on translation, RNA synthesis, and viral replication. Virology **339:**200–212.
3. **Arias, C. F., F. Preugschat, and J. H. Strauss.** 1993. Dengue 2 virus NS2B and NS3 form a stable complex that can cleave NS3 within the helicase domain. Virology **193:**888–899.
4. **Backes, B. J., J. L. Harris, F. Leonetti, C. S. Craik, and J. A. Ellman.** 2000. Synthesis of positional-scanning libraries of fluorogenic peptide substrates to define the extended substrate specificity of plasmin and thrombin. Nat. Biotechnol. **18:**187–193.
5. **Bazan, J. F., and R. J. Fletterick.** 1989. Detection of a trypsin-like serine protease domain in flaviviruses and pestiviruses. Virology **171:**637–639.
6. **Blanchard, J. E., N. H. Elowe, C. Huitema, P. D. Fortin, J. D. Cechetto, L. D. Eltis, and E. D. Brown.** 2004. High-throughput screening identifies inhibitors of the SARS coronavirus main proteinase. Chem. Biol. **11:**1445–1453.
7. **Brinton, M. A.** 2002. The molecular biology of West Nile virus: a new invader of the Western Hemisphere. Annu. Rev. Microbiol. **56:**371–402.
8. **Chambers, T. J., A. Grakoui, and C. M. Rice.** 1991. Processing of the yellow fever virus nonstructural polyprotein: a catalytically active NS3 proteinase domain and NS2B are required for cleavages at dibasic sites. J. Virol. **65:** 6042–6050.
9. **Chambers, T. J., A. Nestorowicz, S. M. Amberg, and C. M. Rice.** 1993. Mutagenesis of the yellow fever virus NS2B protein: effects on proteolytic processing, NS2B-NS3 complex formation, and viral replication. J. Virol. **67:**6797–6807.
10. **Chappell, K. J., M. J. Stoermer, D. P. Fairlie, and P. R. Young.** 2006. Insights to substrate binding and processing by West Nile Virus NS3 protease through combined modeling, protease mutagenesis, and kinetic studies. J. Biol. Chem. **281:**38448–38458.
11. **Cheng, T. J., A. Brik, C. H. Wong, and C. C. Kan.** 2004. Model system for high-throughput screening of novel human immunodeficiency virus protease inhibitors in *Escherichia coli*. Antimicrob. Agents Chemother. **48:**2437–2447.
12. **Clum, S., K. E. Ebner, and R. Padmanabhan.** 1997. Cotranslational membrane insertion of the serine proteinase precursor NS2B-NS3(Pro) of dengue virus type 2 is required for efficient in vitro processing and is mediated through the hydrophobic regions of NS2B. J. Biol. Chem. **272:**30715–30723.
13. **Erbel, P., N. Schiering, A. D'Arcy, M. Renatus, M. Kroemer, S. P. Lim, Z. Yin, T. H. Keller, S. G. Vasudevan, and U. Hommel.** 2006. Structural basis for the activation of flaviviral NS3 proteases from dengue and West Nile virus. Nat. Struct. Mol. Biol. **13:**372–373.
14. **Falgout, B., R. H. Miller, and C.-J. Lai.** 1993. Deletion analysis of dengue virus type 4 nonstructural protein NS2B: identification of a domain required for NS2B-NS3 protease activity. J. Virol. **67:**2034–2042.
15. **Falgout, B., M. Pethel, Y. M. Zhang, and C. J. Lai.** 1991. Both nonstructural proteins NS2B and NS3 are required for the proteolytic processing of dengue virus nonstructural proteins. J. Virol. **65:**2467–2475.
16. **Halstead, S. B.** 2002. Dengue. Curr. Opin. Infect. Dis. **15:**471–476.
17. **Holden, K. L., D. A. Stein, T. C. Pierson, A. A. Ahmed, K. Clyde, P. L. Iversen, and E. Harris.** 2006. Inhibition of dengue virus translation and RNA synthesis by a morpholino oligomer targeted to the top of the terminal 3′ stem-loop structure. Virology **344:**439–452.
18. **Johnston, P. A., J. Phillips, T. Y. Shun, S. Shinde, J. S. Lazo, D. M. Huryn, M. C. Myers, B. I. Ratnikov, J. W. Smith, Y. Su, R. Dahl, N. D. Cosford, S. A. Shiryaev, and A. Y. Strongin.** 2007. HTS identifies novel and specific uncompetitive inhibitors of the two-component NS2B-NS3 proteinase of West Nile virus. Assay Drug Dev. Technol. **5:**737–750.
19. **Jones, C. T., C. G. Patkar, and R. J. Kuhn.** 2005. Construction and applications of yellow fever virus replicons. Virology **331:**247–259.
20. **Jones, M., A. Davidson, L. Hibbert, P. Gruenwald, J. Schlaak, S. Ball, G. R. Foster, and M. Jacobs.** 2005. Dengue virus inhibits alpha interferon signaling by reducing STAT2 expression. J. Virol. **79:**5414–5420.
21. **Khromykh, A. A., and E. G. Westaway.** 1997. Subgenomic replicons of the flavivirus Kunjin: construction and applications. J. Virol. **71:**1497–1505.
22. **Li, H., S. Clum, S. You, K. E. Ebner, and R. Padmanabhan.** 1999. The serine protease and RNA-stimulated nucleoside triphosphatase and RNA helicase domains of dengue virus type 2 NS3 converge within a region of 20 amino acids. J. Virol. **73:**3108–3116.
23. **Lindenbach, B. D., and C. M. Rice.** 2003. Molecular biology of flaviviruses. Adv. Virus Res. **59:**23–61.
24. **Lipinski, C. A., F. Lombardo, B. W. Dominy, and P. J. Feeney.** 2001. Experimental and computational approaches to estimate solubility and permeabil-

ity in drug discovery and development settings. Adv. Drug. Deliv. Rev. **46:**3–26.

25. **Lo, M. K., M. Tilgner, and P. Y. Shi.** 2003. Potential high-throughput assay for screening inhibitors of West Nile virus replication. J. Virol. **77:**12901–12906.
26. **Monath, T. P., and F. X. Heinz.** 1996. Flaviviruses, p. 961–1034. *In* B. N. Fields, D. M. Knipe, and P. M. Howley (ed.), Fields virology. Lippincott-Raven, Philadelphia, PA.
27. **Mueller, N. H., C. Yon, V. K. Ganesh, and R. Padmanabhan.** 2007. Characterization of the West Nile virus protease substrate specificity and inhibitors. Int. J. Biochem. Cell Biol. **39:**606–614.
28. **Pierson, T. C., M. D. Sanchez, B. A. Puffer, A. A. Ahmed, B. J. Geiss, L. E. Valentine, L. A. Altamura, M. S. Diamond, and R. W. Doms.** 2006. A rapid and quantitative assay for measuring antibody-mediated neutralization of West Nile virus infection. Virology **346:**53–65.
29. **Puig-Basagoiti, F., T. S. Deas, P. Ren, M. Tilgner, D. M. Ferguson, and P. Y. Shi.** 2005. High-throughput assays using a luciferase-expressing replicon, virus-like particles, and full-length virus for West Nile virus drug discovery. Antimicrob. Agents Chemother. **49:**4980–4988.
30. **Rice, C. M., E. M. Lenches, S. R. Eddy, S. J. Shin, R. L. Sheets, and J. H. Strauss.** 1985. Nucleotide sequence of yellow fever virus: implications for flavivirus gene expression and evolution. Science **229:**726–733.
31. **Sarubbi, E., M. L. Nolli, F. Andronico, S. Stella, G. Saddler, E. Selva, A. Siccardi, and M. Denaro.** 1991. A high throughput assay for inhibitors of HIV-1 protease. Screening of microbial metabolites. FEBS Lett. **279:**265–269.
32. **Shi, P. Y., M. Tilgner, and M. K. Lo.** 2002. Construction and characterization of subgenomic replicons of New York strain of West Nile virus. Virology **296:**219–233.
33. **Wengler, G., G. Czaya, P. M. Farber, and J. H. Hegemann.** 1991. In vitro synthesis of West Nile virus proteins indicates that the amino-terminal segment of the NS3 protein contains the active centre of the protease which cleaves the viral polyprotein after multiple basic amino acids. J. Gen. Virol. **72:**851–858.
34. **Yusof, R., S. Clum, M. Wetzel, H. M. Murthy, and R. Padmanabhan.** 2000. Purified NS2B/NS3 serine protease of dengue virus type 2 exhibits cofactor NS2B dependence for cleavage of substrates with dibasic amino acids in vitro. J. Biol. Chem. **275:**9963–9969.
35. **Zhang, L., P. M. Mohan, and R. Padmanabhan.** 1992. Processing and localization of dengue virus type 2 polyprotein precursor NS3-NS4A-NS4B-NS5. J. Virol. **66:**7549–7554.